Journal of Hydrology 544 (2017) 319–326

Contents lists available at ScienceDirect

Journal of Hydrology

journal homepage: www.elsevier.com/locate/jhydrol

Research papers

Concurrent temporal stability of the apparent electrical conductivity and soil water content

Aura Pedrera-Parrilla [a,*], Yakov A. Pachepsky [b], Encarnación V. Taguas [c], Sergio Martos-Rosillo [d], Juan V. Giráldez [e,f], Karl Vanderlinden [a]

[a] IFAPA, Centro Las Torres-Tomejil, Ctra. Sevilla-Cazalla km 12.2, 41200 Alcalá del Río (Sevilla), Spain
[b] Environmental Microbial and Food Safety Lab USDA, ARS, NEA, BARC, EMFSL 10300 Baltimore Avenue, BARC-East Beltsville, MD 20705, United States
[c] Departamento de Ingeniería Rural, Universidad de Córdoba, Campus de Rabanales, Edificio da Vinci. Ctra. Madrid km 396, 14071 Córdoba, Spain
[d] Department of Geosciences Research and Prospective, Geological Survey of Spain, Calle de Ríos Rosas 23, 28003 Madrid, Spain
[e] Departamento de Agronomía, Universidad de Córdoba, Campus de Rabanales, Edificio da Vinci. Ctra. Madrid km 396, 14071 Córdoba, Spain
[f] Instituto de Agricultura Sostenible, CSIC, Avda. Menéndez Pidal s/n, 14080 Córdoba, Spain

ARTICLE INFO

Article history:
Received 1 December 2015
Received in revised form 4 October 2016
Accepted 11 October 2016
Available online 19 October 2016
This manuscript was handled by Peter K. Kitanidis, Editor-in-Chief, with the assistance of Nunzio Romano, Associate Editor

Keywords:
Soil-water content
Apparent electrical conductivity
Temporal stability
Soil spatial classification

ABSTRACT

Knowledge of spatio-temporal soil-water content (SWC) variability in agricultural fields is useful for improving crop management. Spatial patterns of SWC can be characterized using temporal stability analysis of difficult-to-obtain data from high spatial density and temporal frequency. Soil apparent electrical conductivity (ECa) measurements with high spatial density have been widely used to infer the spatial variability of SWC. The objective of this work is to test the hypothesis that temporal stability of ECa can be demonstrated and that relationships between temporal stability characteristics of SWC and ECa can be established. Apparent electrical conductivity and topsoil gravimetric SWC (θ) were periodically measured in an olive orchard in southwest Spain on 6 and 18 occasions, respectively. A temporal stability analysis of ECa elucidated three zones where ECa was close to, consistently substantially smaller than, and substantially larger than the spatial average ECa throughout the study period. Representative locations for θ were found with a chance of 75% within the representative zone for ECa. Yet, the driest locations, with consistently smaller θ than the field average ($\langle\theta\rangle$), could be successfully identified (89%) within the zone with consistently smaller ECa than average. The $\theta - \langle\theta\rangle$ relations showed generally a linear behaviour, although a better fit was obtained at the highest θ using either exponential or power law equations at half of the locations. The former provided the best fit within the zone with ECa consistently smaller than average, while the latter performed best in the zone with ECa consistently larger than average. The linear equation provided the best fit within the representative ECa zone. This study demonstrates that temporal stability characteristics of ECa and SWC are linked and that ECa surveys can be used to delimit zones with representative locations for SWC measurement or estimation. Such information is of importance for a range of agricultural applications, *i.e.* irrigation, crop protection, fertilizer management, and soil and water conservation.

© 2016 Elsevier B.V. All rights reserved.

1. Introduction

Knowledge of spatio-temporal variability of soil-water content (SWC) at the field scale is useful for improving soil and water conservation practices, for efficient irrigation management and scheduling, and for reducing contamination of surface and ground water by fertilizers and pesticides (Hupet and Vanclooster, 2002; Brocca et al., 2009). Spatial patterns of the field SWC often exhibit temporal stability, *i.e.* locations can be identified where the soil is consistently dryer or consistently wetter than the field average SWC, resulting in a persisting bias (Vanderlinden et al., 2012; Vereecken et al., 2014). This information can be used to delimit zones within fields where different management strategies can be implemented (Kaleita et al., 2007). Spatially and temporally dense SWC sampling is needed to perform such zonation.

Spatial patterns of SWC are difficult to infer since high-density SWC monitoring with sensor networks (Vereecken et al., 2014) remains expensive and the required field equipment generally

* Corresponding author.
E-mail addresses: aura.pedrera@juntadeandalucia.es (A. Pedrera-Parrilla), yakov.pachepsky@ars.usda.gov (Y.A. Pachepsky), ir2tarue@uco.es (E.V. Taguas), s.martos@igme.es (S. Martos-Rosillo), ag1gicej@uco.es (J.V. Giráldez), karl.vanderlinden@juntadeandalucia.es (K. Vanderlinden).

http://dx.doi.org/10.1016/j.jhydrol.2016.10.017
0022-1694/© 2016 Elsevier B.V. All rights reserved.

interferes with common field operations. During the last decade electromagnetic induction (EMI) instruments, which measure the soil apparent electrical conductivity (ECa), have been increasingly used to estimate the spatial variability of SWC (Martínez et al., 2010; Martínez García et al., 2012; Calamita et al., 2015). Apart from SWC, ECa depends also on clay content, solute concentration in the pore water, and temperature (Brevik and Fenton, 2002; Corwin and Lesch, 2005; Friedman, 2005). Spatial variation of these soil properties hampers the efficient SWC mapping using EMI instruments (Martínez García et al., 2012).

Evidence exists that spatial patterns of ECa also exhibit temporal stability (Van Arkel and Kaleita, 2014). Since ECa increases with the increase in SWC and clay content, and SWC increases with the increase in clay content, we hypothesize that the spatial distribution of ECa can be temporally stable if the spatial distribution of SWC is temporally stable, and that ECa and SWC temporal stability parameters may be related.

Currently, data that allow temporal stability of ECa patterns to be demonstrated or deduced are scarce. Available ECa data showed persistently positive or negative deviations from the spatial mean in different zones of study areas (Martínez et al., 2010; Zhu et al., 2010; Van Arkel and Kaleita, 2014). Robinson et al. (2010) reported spatially persistent ECa deviations from the average values. They identified zones of water depletion and accumulation based on the time-lapse ECa imaging. Although accurate relationships between SWC and ECa were difficult to establish using data from individual locations, the authors found that the temporally stable spatial patterns for SWC and ECa were related. Given the feasibility of high density "on-the-go" measurements with EMI instruments (Adamchuk et al., 2004; Doolittle and Brevik, 2014), using the ECa maps presents a promising way to estimate spatial SWC patterns, and to identify representative locations for estimating field-average SWC.

The objectives of this work were to demonstrate that (i) temporal stability of spatial ECa patterns exists, (ii) that relationships between temporal stability characteristics of SWC and ECa can be identified, and that (iii) zones can be delimited where SWC and ECa show a similar deviation from their respective field mean values.

2. Materials and methods

2.1. Site description

The study was performed in the experimental catchment "La Manga" (36°52′21″N, 5°7′44″W) located in Setenil de las Bodegas in the SouthWest of Spain. The mean elevation and slope are 740 m above mean sea level and 10%, respectively (Pedrera-Parrilla et al., 2016). The catchment covers an area of 6.7 ha of a rainfed olive orchard which was planted in 1995 on a 7 × 7-m grid. Trees were under minimum tillage with chemical weed control. The soil subgroup varies between Lithic and Typic Rhodoxeralf (Soil Survey Staff, 1999, pp. 269–270; García del Barrio et al., 1971). The soil texture is loamy sand and the maximum depth to the underlying calcarenite bedrock is 1.2 m. A gully intersects the catchment from SE to NW towards the catchment outlet and separates the two main subareas with different slopes. Throughout the two years of observation, the catchment was tilled 2–3 times/year using a disc harrow. The climate is Mediterranean, with a mean annual precipitation of 700 mm. Rainfall occurs mainly from October to May (75%) as intense and short events. Generally, in these weakly developed soils, the steep topography often induces topsoil water erosion, leading to outcropping of the bedrock and the appearance of zones where the humic-rich horizon rarely exceeds 0.1 m (Taguas and Gómez, 2015).

2.2. Soil-water content

During 2011 and 2012, the field was sampled on 18 days for gravimetric SWC, at 41 locations on a grid using a 0.05-m diameter Edelman auger. Gravimetric SWC for the 0–0.2 m depth range, θ, was obtained as the average of the measured SWC in the 0–0.1 m and the 0.1–0.2 m depth ranges (see Fig. 1).

2.3. Apparent electrical conductivity

ECa surveys were performed with the DUALEM-21S sensor (DUALEM, Milton, Canada). This EMI sensor features one transmitter coil and four receiver coils at distances of 1, 1.1, 2 and 2.1 m from the transmitter coil (Dualem Inc., 2007). Receiver coils are oriented, with respect to the transmitter coil, in the perpendicular (P) or in the horizontal co-planar (H) spatial configuration. The four transmitter-receiver configurations allow the sensor to measure ECa simultaneously in four different soil volumes. The corresponding depth of exploration (DOE), defined as the depth at which 70% of the sensor response is achieved (McNeill, 1980; Callegary et al., 2007), ranged from approximately 0.5 to 3 m.

Six ECa surveys were conducted during 2011 and 2012 (see Fig. 1). Surveys were performed at a speed in the range of 5–10 km/h, with a distance of 7 m between parallel measurement lines, according to the olive row spacing, and with an inline measurement frequency of 1 Hz. After each of the field-wide surveys, ECa was also measured at the 41 SWC sampling locations. The ECa data were filtered and interpolated using the Vesper software package (Whelan et al., 2002) to create maps. We examined the ECa signal from the 1-m H coil configuration, with the DOE of approximately 1.5 m, since this signal provided the best correspondence with the analysed soil variables.

2.4. Data analysis

The temporal stability analysis was performed using the θ measured at the 41 locations during 18 surveys and the interpolated ECa maps for six surveys (Fig. 1). The relative differences (RD),

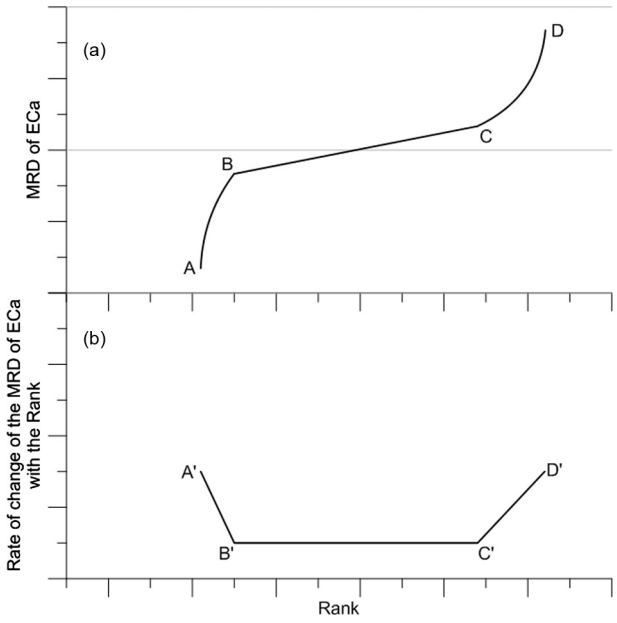

Fig. 1. Schematic representation of (a) a rank stability plot of mean relative difference (MRD) of apparent electrical conductivity (ECa) and (b) of the rate of change of the MRD with the rank.

the mean of the relative differences (MRD) and the standard deviation of the relative differences (SDRD), as proposed by Vachaud et al. (1985), were calculated as

$$RD_{ij} = (X_{ij} - \langle X \rangle_j)/\langle X \rangle_j, \quad (1)$$

$$MRD_i = \frac{1}{N}\sum_{j=1}^{j=N} RD_{ij}, \quad (2)$$

and

$$SDRD_i = \sqrt{\frac{1}{N-1}\sum_{j=1}^{j=N}(RD_{ij} - MRD_i)^2}, \quad (3)$$

where i stands for location, j for the survey number, X for θ or ECa, $\langle X \rangle$ for the spatial average, and N for the number of surveys.

MRD and SDRD values are frequently applied in combination to select representative locations for the spatial average SWC throughout the study period, with MRD ≈ 0 and minimum SDRD (Guber et al., 2008; Schneider et al., 2008; Vanderlinden et al., 2012; Vereecken et al., 2014).

To classify the MRD values spatially, the following procedure was used. Fig. 2a shows schematically a rank stability plot for ECa (MRD versus rank). Three different regions (A-B, B-C, and C-D) were delimited by considering the rate of change of the MRD of ECa with the rank (Fig. 2b). The rate was calculated as the first derivative of the rank-stability plot of ECa MRD. The ECa MRD map was then classified into three regions shown in Fig. 3. Based on this information, the correspondence between SWC MRD and ECa MRD within the different ECa zones was analysed.

Representative locations are defined as locations where measurements can be used either directly or transformed to accurately represent the average SWC. Removal of bias in locations with small SDRD was proposed as a way to find candidate representative locations (Starks et al., 2006; Heathman et al., 2009). If bias removal is sufficient to estimate the field average, then the linear relationship is expected to exist between SWC measured at a single location and the field-average spatial SWC, with a slope close to 1:1. At each of the 41 locations the relationships between SWC and the corresponding spatial average were also studied. Linear, exponential, and power-law equations were fitted to these relationships. Since those equations have different numbers of parameters, the Akaike Information Criterion (AIC) (Akaike, 1974) was used to compare the goodness-of-fit. The AIC relates the number of model parameters k to the goodness of fit:

$$\mathrm{AIC} = 2k - 2\ln(L), \quad (4)$$

where L the likelihood function for the prediction model.

For small sample sizes of this work, the following correction was applied:

$$\mathrm{AIC_c} = AIC + 2k(k+1)/(n-k-1), \quad (5)$$

where n is the number of prediction data (Burnham and Anderson, 2002).

3. Results

3.1. Preliminary data analysis

Fig. 1 shows that in the top 0–0.2 m $\langle\theta\rangle$ reached values near 0.02 kg kg^{-1} during the summer (surveys 7–9, 15, and 16). These small $\langle\theta\rangle$ values were overall associated with the largest CVs, ranging from 34 to 52%. The $\langle\theta\rangle$ was larger than 0.11 kg kg^{-1} during wet periods (surveys 1, 2, 4, 10, 11, 13, 17, and 18). The larger $\langle\theta\rangle$ values were associated with the smallest CVs, ranging from 13 to 19%.

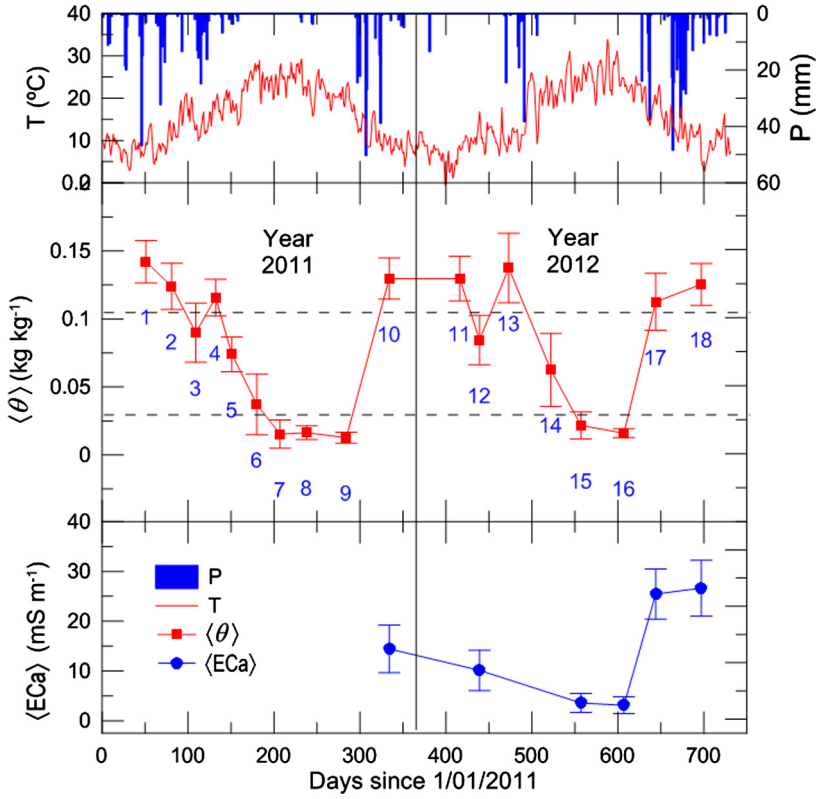

Fig. 2. Time series of air temperature (T), precipitation (P), spatially averaged gravimetric topsoil (0–0.2 m) water content ($\langle\theta\rangle$), and spatially averaged apparent electrical conductivity ($\langle$ECa$\rangle$), measured at 41 locations during 2011 and 2012. Error bars represent standard deviations. Dashed lines correspond to values of 0.11 and 0.02 kg kg^{-1} and represent the limit between large and intermediate $\langle\theta\rangle$ and intermediate and small $\langle\theta\rangle$.

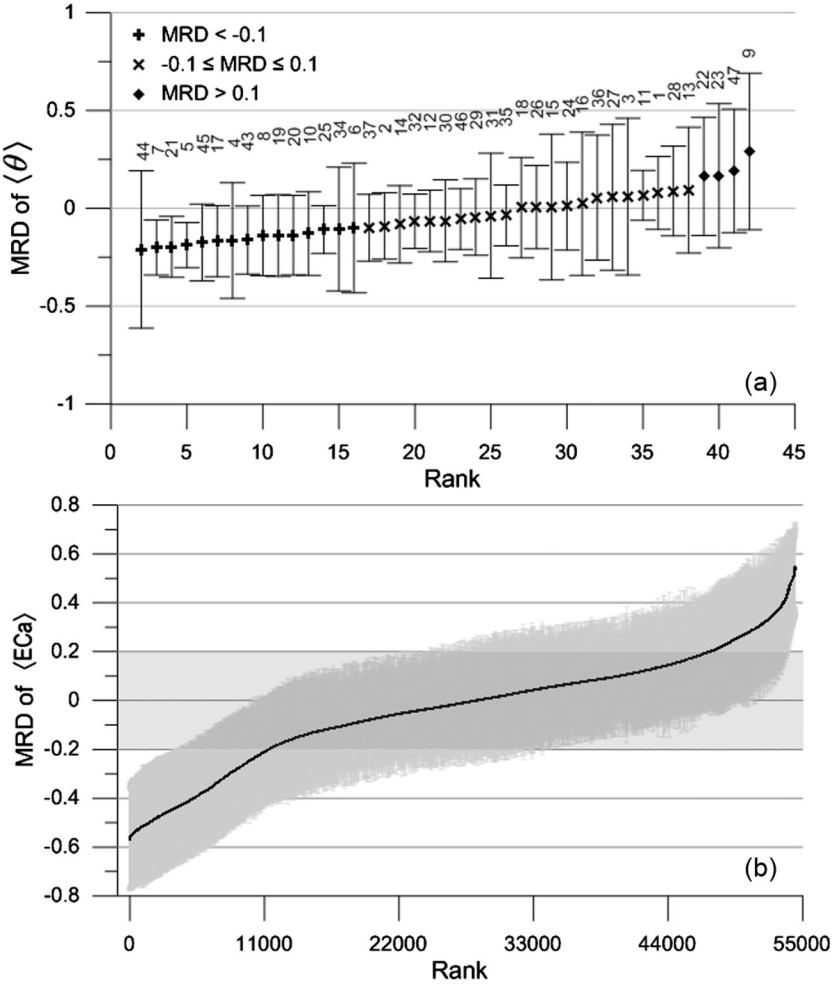

Fig. 3. Rank stability plots of (a) mean relative differences (MRDs) of gravimetric topsoil (0–0.2 m) water content (θ), and (b) apparent electrical conductivity (ECa).

Surveys 3, 5, 6, 12, and 14 ($0.11 > SWC > 0.02$ kg kg^{-1}) showed intermediate $\langle\theta\rangle$ and CVs. Similarly, large $\langle$ECa$\rangle$ values corresponded to smaller CVs and vice versa (Fig. 1). Surveys 10 and 12 showed intermediate $\langle$ECa$\rangle$ values and CVs of 33 and 40%, respectively. Surveys 15 and 16 presented the smallest $\langle$ECa$\rangle$ and CVs of 53 and 54%, respectively. The largest $\langle$ECa$\rangle$ was observed in surveys 17 and 18, with a CV of 20% for both cases. The similarities observed in the spatio-temporal organization of θ and ECa are indicative of the link that exists between both, and of the existence of concurrent temporal stability of ECa and θ.

3.2. Temporal stability of SWC and ECa

Rank stability plots of θ and ECa are shown in Fig. 3. The range of θ MRD was about 0.5 (Fig. 3a). Accordingly, an interval of ±0.1 was chosen to delineate locations with a MRD close to zero. Approximately half of the locations (46%) were outside this interval. MRD values were above 0.1 and below −0.1 in 10% and 36% of locations, respectively. The range of ECa MRD was approximately 1, *i.e.* twice the range of θ MRD. The ECa rank stability plot (Fig. 3b) showed two well-defined regions of change of slope. These regions were delimited using the corresponding derivative (Fig. S1). At the lower ECa MRD end, corresponding to the A′-B′ region, the change in slope occurred roughly between ranks ranging from 10,000 to 15,000. At the higher ECa MRD end, corresponding to the C′-D′ region, a strong change in slope was observed between ranks ranging from 45,000 to 52,000. To identify the centers of these regions of changing slope, the average rank within each region was calculated (stars in Fig. S1). These average ranks corresponded roughly to ECa MRD values near −0.2 and 0.2 *i.e.* twice the interval of θ MRD. Locations with ECa MRD within the interval of ±0.2 were therefore designated as locations with a MRDs close to zero. From a total of 54,388 ECa measurement locations, 33% were outside the interval ±0.2, with 12 and 21% above 0.2 and below −0.2, respectively. The corresponding SDRD is represented by error bars in Fig. 3a and by the shaded are in Fig. 3b, and was on average approximately 0.3 for both ECa and θ.

3.3. Spatial pattern of SWC and ECa

The ECa MRD map (Fig. 4a) showed that for a large portion of the catchment MRD was close to zero ($-0.2 \leqslant MRD \leqslant 0.2$). ECa measurements at locations within this zone can be considered representative of the spatial mean ECa, while locations within the $MRD < -0.2$ and $MRD > 0.2$ zones provided consistently lower and higher ECa values than the spatial mean, respectively.

The spatial θ MRD distribution (Fig. 4b) showed substantial similarity to the ECa MRD spatial distribution. We investigated the effect of the selection of MRD ranges on the overlap of zones with different temporal stability for θ and ECa (Table 1). Percentages of overlap of θ and ECa zones with MRDs close to the spatial mean ranged from 61 to 85%. Percentages of overlap of zones with ECa MRD values below −0.15, −0.2, and −0.25 and θ MRD below −0.075, −0.1, and −0.125, respectively, ranged from 89 to 100%.

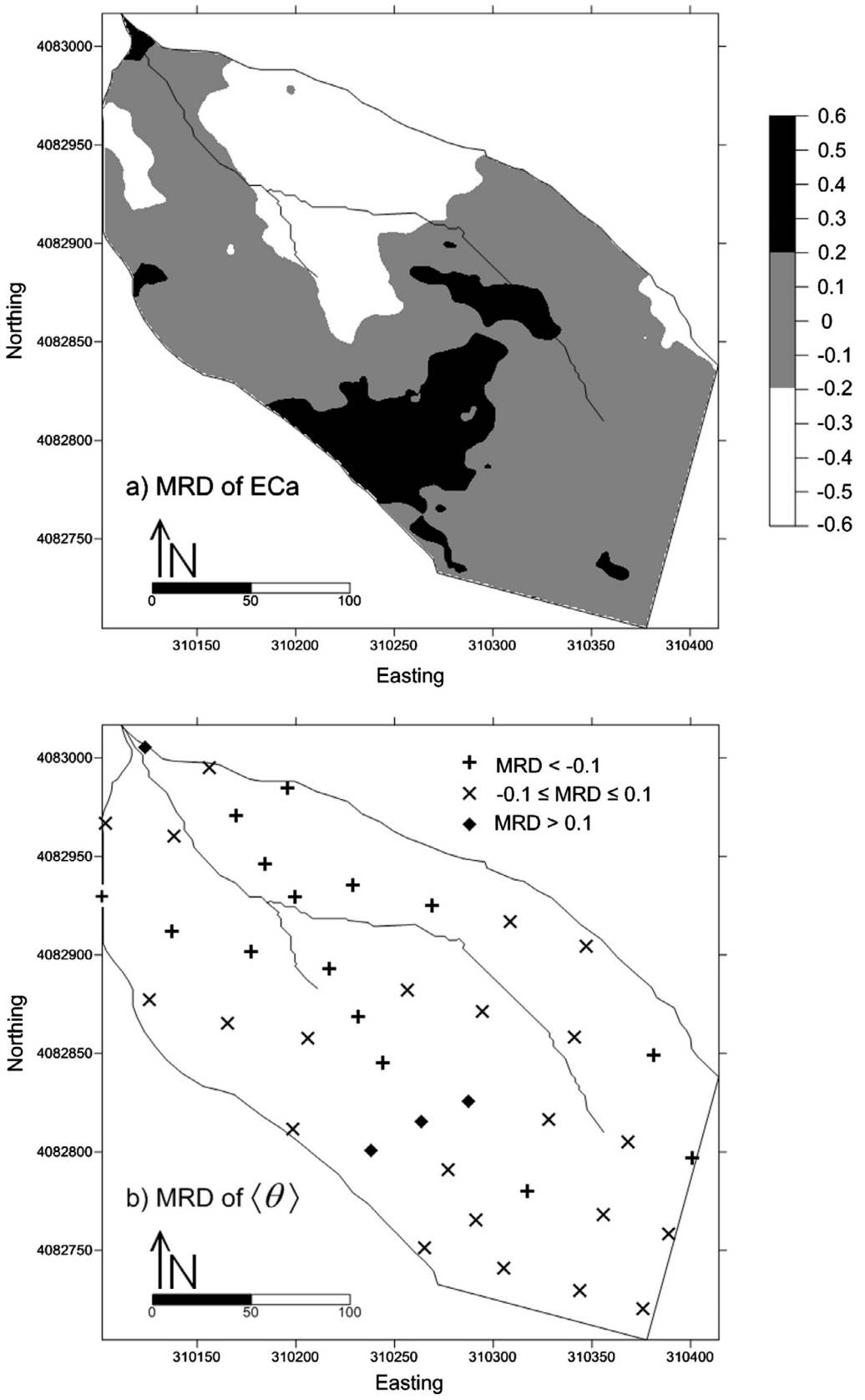

Fig. 4. Spatial distribution of the mean relative difference (MRD) of (a) apparent electrical conductivity (ECa) and (b) gravimetric topsoil (0–0.2 m) water content (θ) in the study area.

Table 1
Probability (%) of overlap between zones with three different mean relative difference (MRD) ranges of soil-water content (SWC) and apparent electrical conductivity (ECa).

		ECa		
		MRD < (−0.25)	(−0.25) ⩽ MRD ⩽ 0.25	MRD > 0.25
SWC	MRD < (−0.125)	100	15.38	0
	(−0.125) ⩽ MRD ⩽ 0.125	0	84.61	42.85
	MRD > 0.125	0	0	57.14
		ECa		
		MRD < (−0.2)	(−0.2) ⩽ MRD ⩽ 0.2	MRD > 0.2
SWC	MRD < (−0.1)	88.9	25	0
	(−0.1) ⩽ MRD ⩽ 0.1	11.1	75	50
	MRD > 0.1	0	0	50
		ECa		
		MRD < (−0.15)	(−0.15) ⩽ MRD ⩽ 0.15	MRD > 0.15
SWC	MRD < (−0.075)	100	33.33	0
	(−0.1) ⩽ MRD ⩽ 0. 075	0	61.11	50
	MRD > 0. 075	0	5.55	50

Finally, at least 50% overlap was found for zones with ECa MRD values above 0.15, 0.2, and 0.25 and θ MRD above 0.075, 0.1, and 0.125, respectively. The probability of spatial overlap for locations of θ and zones of ECa, in terms of MRDs was 89% for ECa MRD < −0.2, 75% for MRDs close to the spatial mean (−0.2 ⩽ ECa MRD ⩽ 0.2), and 50% for ECa MRD > 0.2.

3.4. Relationships between point values and spatial means

Linear regressions were computed using the point values as the independent variable and the spatial averages as the dependent variable. Coefficients of correlation ranged from 0.87 to 0.99, and the slopes (m) ranged from 0.81 to 1.2. At some locations, non-linear relationships were observed between θ and $\langle\theta\rangle$. Examples of such relationships are shown in Fig. 5 for each of the three zones delimited on the ECa MRD map (Fig. 4a). Fig. 5 shows that at location 7, which is representative for ECa MRD < −0.2, the deviation between θ and $\langle\theta\rangle$ ($\theta - \langle\theta\rangle$) decreased with $\langle\theta\rangle$ up to a $\langle\theta\rangle$ threshold from which the deviation became again close to zero. At location 32, which is representative for −0.2 ⩽ ECa MRD ⩽ 0.2, deviations are close to zero over the entire $\langle\theta\rangle$ range, while at location 23, which is representative for ECa MRD > 0.2, $\theta - \langle\theta\rangle$ increases with $\langle\theta\rangle$. According to the AICc (Eq. (5), Table S1), either power law (10%) or exponential (39%) equations provided best fits at nearly half of the sampling locations. For example, the exponential equation was the best for the data from location 7 (Fig. S2a). Exponential relationships are indicative of the existence of the upper limit for $\langle\theta\rangle$, while θ can further increase beyond this threshold. The linear relationship was the best for the location 32 where θ was close to $\langle\theta\rangle$ over the entire $\langle\theta\rangle$ range. The slope m values lower than 1 correspond to locations with progressively smaller θ than $\langle\theta\rangle$, whereas m values higher than 1 indicated the opposite trend, *i.e.* progressively larger θ than $\langle\theta\rangle$. The power-law relationship was found more suitable for the location 23 data. Approximately half (24 out of 41) of the locations in which the linear model was deemed acceptable still showed a slight deviation from linearity for the highest $\langle\theta\rangle$ (*e.g.* location 30, Fig. 6).

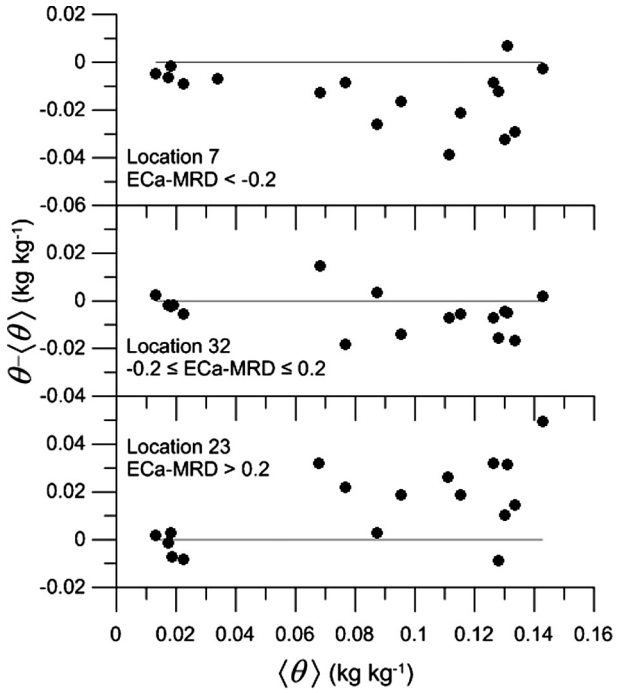

Fig. 5. Relationships between gravimetric topsoil (0–0.2 m) water content deviations from the spatial average ($\theta - \langle\theta\rangle$) and $\langle\theta\rangle$ at locations 7, 32, and 23.

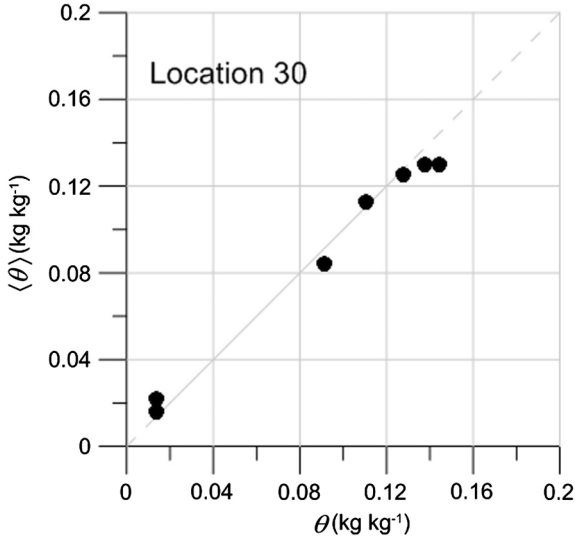

Fig. 6. Relationship between point values (θ) and the spatial average of gravimetric topsoil (0–0.2 m) water content ($\langle\theta\rangle$) at location 30 for 2011.

4. Discussion

The temporal-stability analysis for θ and ECa showed stable patterns for both soil properties (Fig. 3). The range of ECa MRD was more than twice the range of θ MRD probably because there are soil properties other than θ that also influence ECa. The SDRD was proportional to MRD across the entire range of MRD. Unlike ranges of MRD, ranges of SDRD for ECa and θ were similar. Therefore, the ratios of SDRD range to MRD range were smaller for ECa than for θ. One possible reason is the difference between the soil volumes explored by the measurement methods of the two variables. The value of θ was measured in the topsoil (0–0.2 m), whereas the ECa measurements reflected a distribution of soil properties throughout the entire soil profile. We did not find literature on the temporal stability of SWC in soil layers of different thicknesses. Yet, literature data on the temporal stability of SWC for different depths is available, and show changes in SWC MRD ranges with depth. While MRD values did not change significantly with depth (Martínez et al., 2010; Liu and Shao, 2014), some studies reported increasing SDRD of SWC and others found decreasing SDRD with soil depth (Hu et al., 2010; Choi and Jacobs, 2011). The effect of soil depth on the temporal stability of ECa has not been studied so far.

Shapes of the rank-stability plot for θ (Fig. 3) were similar to those found in previous works (Vachaud et al., 1985; Cosh et al., 2006; Herbst et al., 2009; Martínez et al., 2010; Vanderlinden et al., 2012). They are characterized by a positive and approximately linear trend for values of MRD that are negative and close to zero, and a non-linear increase for the largest MRDs. The rank stability plots of ECa and θ showed a somewhat different shape. The rank stability plot for ECa was more symmetrical and showed curvilinear dependencies of MRD on rank where the absolute values of the MRDs substantially deviated from zero.

There was substantial overlap between zones where representative locations for ECa and θ could be found (Fig. 4). The probability for the same location to be representative of the spatial mean of θ and ECa, considering MRDs within ranges of ±0.1 and ±0.2, respectively, was 75%. This probability increased up to 89% for the driest locations with the lowest MRD values. A change in these MRD ranges can affect the percentage of overlap (Table 1). The range of ECa MRD ±0.2 showed the highest percentages of overlap for the three zones (89, 75 and 50%), and particularly for the ECa MRD > 0.2 zone. These results indicate that information on ECa can be relevant for a range of agricultural applications such as irrigation and crop and soil management. ECa surveys can help to identify locations that are representative for the field-average SWC and locations that are persistently drier than the field-average. Depending on the chosen irrigation strategy, soil moisture sensors for irrigation scheduling can then be installed at these locations. Similar applications exist with respect to crop protection, fertilization, or the implementation of soil and water conservation techniques.

One way to define a representative location is to select a location with small SDRD and use the MRD value as a constant bias to acquire the average SWC over the observation area (Starks et al., 2006; Heathman et al., 2009). Candidate representative locations should show SWC deviations from the field-average that are independent from that field-average SWC. Fig. 5 shows that this only occurs in the zone with small absolute values of ECa MRD (central panel in Fig. 5). In the zones with large absolute ECa MRD the deviation of θ from $\langle\theta\rangle$ depends on $\langle\theta\rangle$, and the relationship between θ and $\langle\theta\rangle$ becomes nonlinear (Fig. S2). The information theory-based model (performance criterion AICc) indicated that in the latter zones, accounting for approximately half of the sampling locations, power law and exponential models fitted better the $\theta - \langle\theta\rangle$ relationships than the linear model (see also Fig. S2). When considering ECa, the equivalent relationships were best modelled by linear relationships across the entire study area.

Even when linear relationships were found to be applicable, slight deviations from linearity were observed for the highest $\langle\theta\rangle$ (*e.g.* Fig. 6). It is possible that the deviations from linearity become even larger when the soil is wetter than shown in Fig. 6. We do not know why such nonlinearity occurs. One potential explanation is that measurements of θ and ECa cover different ranges of soil depth. It is possible that storage in the entire soil column is more temporally stable than the water content in the top 0–0.2 m layer. Vanderlinden et al. (2012) found that for soil depths <0.5 m intermediate SWC SDRD values (roughly between 0.1 and 0.3) are commonly found, while SDRDs outside of this range can occur for all depths. This was explained by the effect of vegetation and agricultural activity (*e.g.* tillage). Another reason may be the combined effects of soil texture and topography. The modified Archie's law for unsaturated materials (Frohlich and Parke, 1989) accounts for an additional term for apparent surface resistivity. Larger clay contents can lead to larger SWCs and thus to larger non-linearity. Spatial variations of clay and gravel content, and soil depth, in addition to the fact that only topsoil SWC can be measured in this particular field, may interact with each other and cause these non-linear trends. Lower clay contents and higher gravel contents, which were found to be located in the shallow soil area at the NE part of the field in previous studies (Pedrera-Parrilla et al., 2016), led to smaller θ as compared to $\langle\theta\rangle$ at intermediate $\langle\theta\rangle$. The soil depth of the test site ranged from 0.1 to 1.2 m, with a calcareous rock underneath, also affecting the infiltration and evaporation processes in the topsoil. This surely is a topic for further research. Overall, in shallow soils with significant spatial differences in soil properties, the estimation of $\langle\theta\rangle$ via the addition of the corresponding bias may be not a valid approach.

Locations with non-linear (power law and exponential) dependencies were not suitable to represent $\langle\theta\rangle$, even after the bias was removed. It appears that not only MRD and SDRD, but also the dependencies of absolute differences of θ with $\langle\theta\rangle$ can be used to guide the selection of representative locations for SWC in shallow soils with variable soil depth and significant spatial variations in soil properties and topography.

5. Conclusions

Spatial patterns of θ and ECa exhibited temporal stability and representative locations for their respective spatial averages could be identified. All θ sampling locations provided satisfactory linear relationships with $\langle\theta\rangle$, although at approximately half of these locations non-linear tendencies were observed for the largest $\langle\theta\rangle$, corresponding mainly to zones for which $-0.2 \geqslant$ ECa MRD $\geqslant 0.2$. Particularly, in zones with ECa MRD < -0.2, where negative deviations from the field-average $(\theta - \langle\theta\rangle)$ increased as the soil became wetter, a better fit between θ and $\langle\theta\rangle$ was provided by an exponential equation. A power-law equation was found more appropriate for zones with ECa MRD > 0.2, where positive deviations from the field-average $(\theta - \langle\theta\rangle)$ increased as the soil became wetter. It is not clear why this on-linearity occurs. The inclusion of the additional surveys, performed under wetter field conditions, could confirm the observed tendencies. The non-linear behaviour between point measurements and the spatial average was not observed for ECa.

In this field, ECa surveys were useful for identifying representative locations for the estimation of $\langle\theta\rangle$. An overlap of 75% between representative locations for θ and representative zones for ECa was found. Yet, information on ECa was most indicated for identifying the driest locations in the field, with consistently smaller θ than

$\langle\theta\rangle$. An agreement of 89% was found between locations that were persistently drier than the field average (θ MRD < −0.1) and regions with persistently smaller ECa (ECa MRD < −0.2).

Our findings show that temporal stability characteristics revealed by ECa surveys can be used to infer information on the temporal stability characteristics of SWC. This opens an avenue for identifying representative SWC monitoring locations within a field without the need to monitor first SWC at a large number of locations. This kind of information provided by ECa surveys is therefore relevant for a range of agricultural applications where knowledge on the spatial distributions of SWC is important (*e.g.* irrigation).

Acknowledgements

Funding for this work came from the Spanish Ministry of Economy and Competitiveness and FEDER (Grants AGL2012-40128-C03-03 and AGL2015-65036-C3-3-R, MINECO/FEDER, EU), and from the Junta de Andalucía (P11-AGR-7431). Also support through PhD grant n° 8 (Res. 15/04/2010) and grant PP.AVA. AVA201601.13 by IFAPA/FEDER is acknowledged. Special thanks to A.J. Espejo, M. Morón, J. García, M.A. Ayala, A. Jardúo and E. Rodríguez of IFAPA Centro Las Torres-Tomejil for their assistance with the field and laboratory work. We are also very grateful to Alonso Zamudio, the owner of the "La Manga" farm, and the staff for their continuous support.

Appendix A. Supplementary material

Supplementary data associated with this article can be found, in the online version, at http://dx.doi.org/10.1016/j.jhydrol.2016.10.017.

References

Adamchuk, V.I., Hummel, J.W., Morgan, M.T., Upadhyaya, S.K., 2004. On-the-go soil sensors for precision agriculture. Comput. Electron. Agric. 44, 71–91. http://dx.doi.org/10.1016/j.compag.2004.03.002.

Akaike, H., 1974. A new look at the statistical model identification. IEEE Trans. Autom. Control 19, 716–723. http://dx.doi.org/10.1109/TAC.1974.1100705.

Brevik, E.C., Fenton, T.E., 2002. Influence of soil water content, clay, temperature, and carbonate minerals on electrical conductivity readings taken with an EM-38. Soil Surv. Horiz. 43, 9–13.

Brocca, L., Melone, F., Moramarco, T., Morbidelli, R., 2009. Soil moisture temporal stability over experimental areas in Central Italy. Geoderma 148, 364–374. http://dx.doi.org/10.1016/j.geoderma.2008.11.004.

Burnham, K.P., Anderson, D.R., 2002. Model Selection and Multimodel Inference: A Practical Information-Theoretic Approach. Springer-Verlag. ISBN 0-387-95364-7.

Calamita, G., Perrone, A., Brocca, L., Onorati, B., Manfreda, S., 2015. Field test of a multi-frequency electromagnetic induction sensor for soil moisture monitoring in southern Italy test sites. J. Hydrol. 529, 316–329. http://dx.doi.org/10.1016/j.jhydrol.2015.07.023.

Callegary, J.B., Ferré, T.P.A., Groom, R.W., 2007. Vertical spatial sensitivity and exploration depth of low-induction-number electromagnetic-induction instruments. Vadose Zone J. 6, 158. http://dx.doi.org/10.2136/vzj2006.0120.

Choi, M., Jacobs, J.M., 2011. Spatial soil moisture scaling structure during soil moisture experiment 2005. Hydrol. Process. 25, 926–932. http://dx.doi.org/10.1002/hyp.7877.

Corwin, D.L., Lesch, S.M., 2005. Characterizing soil spatial variability with apparent soil electrical conductivity: I. Survey protocols. Comput. Electron. Agric. 46, 103–133. http://dx.doi.org/10.1016/j.compag.2004.11.002.

Cosh, M.H., Jackson, T.J., Starks, P., Heathman, G., 2006. Temporal stability of surface soil moisture in the Little Washita River watershed and its applications in satellite soil moisture product validation. J. Hydrol. 323, 168–177. http://dx.doi.org/10.1016/j.jhydrol.2005.08.020.

Doolittle, J.A., Brevik, E.C., 2014. The use of electromagnetic induction techniques in soils studies. Geoderma 223–225, 33–45. http://dx.doi.org/10.1016/j.geoderma.2014.01.027.

Dualem Inc., 2007. DUALEM-21S User's Manual. Dualem Inc., Milton. Canada.

Friedman, S.P., 2005. Soil properties influencing apparent electrical conductivity: a review. Comput. Electron. Agric. 46, 45–70. http://dx.doi.org/10.1016/j.compag.2004.11.001.

Frohlich, R.K., Parke, C.D., 1989. The electrical resistivity of the vadose zone-field study. Ground Water 27, 524–530.

García del Barrio, I., Malvárez, L., González, J.I., 1971. Mapas provinciales de suelos. Cádiz. Ministerio de Agricultura, Madrid.

Guber, A.K., Gish, T.J., Pachepsky, Y.A., van Genuchten, M.T., Daughtry, C.S.T., Nicholson, T.J., Cady, R.E., 2008. Temporal stability in soil water content patterns across agricultural fields. Catena 73, 125–133. http://dx.doi.org/10.1016/j.cat- ena.2007.09.010.

Heathman, G.C., Larose, M., Cosh, M.H., Bindlish, R., 2009. Surface and profile soil moisture spatio-temporal analysis during an excessive rainfall period in the Southern Great Plains, USA. Catena 78, 159–169. http://dx.doi.org/10.1016/j.catena.2009.04.002.

Herbst, M., Prolingheuer, N., Graf, A., Huisman, J.A., Weihermüller, L., Vanderborght, J., 2009. Characterization and understanding of bare soil respiration spatial variability at plot scale. Vadose Zone J. 8, 762–771.

Hu, W., Shao, M., Reichardt, K., 2010. Using a new criterion to identify sites for mean soil water storage evaluation. Soil Sci. Soc. Am. J. 74, 762–773. http://dx.doi.org/10.2136/sssaj2009.0235.

Hupet, F., Vanclooster, M., 2002. Intraseasonal dynamics of soil moisture variability within a small agricultural maize cropped field. J. Hydrol. 261, 86–101. http://dx.doi.org/10.1016/S0022-1694(02)00016-1.

Kaleita, A.L., Hirschi, M.C., Tian, L.F., 2007. Field-scale surface soil moisture patterns and their relationship to topographic indices. Trans. ASABE 50, 557–564.

Liu, B., Shao, M., 2014. Estimation of soil water storage using temporal stability in four land uses over 10 years on the Loess Plateau, China. J. Hydrol. 517, 974–984. http://dx.doi.org/10.1016/j.jhydrol.2014.06.003.

Martínez, G., Vanderlinden, K., Giráldez, J.V., Espejo, A.J., Muriel, J.L., 2010. Field-scale soil moisture pattern mapping using electromagnetic induction. Vadose Zone J. 9, 871. http://dx.doi.org/10.2136/vzj2009.0160.

Martínez García, G., Vanderlinden, K., Pachepsky, Y., Giráldez Cervera, J.V., Espejo-Pérez, A.J., 2012. Estimating topsoil water content of clay soils with data from time-lapse electrical conductivity surveys. Soil Sci. 177, 369–376. http://dx.doi.org/10.1097/SS.0b013e31824eda57.

McNeill, J.D., 1980. Electromagnetic Terrain Conductivity Measurement at Low Induction Numbers. Tech. Note TN-6. Geonics Limited, Mississauga, Ontario, Canada.

Pedrera-Parrilla, A., Van De Vijver, E., Van Meirvenne, M., Epejo, A.J., Giráldez, J.V., Vanderlinden, K., 2016. Apparent electrical conductivity measurements in an olive orchard under wet and dry soil conditions: significance for clay and soil water content mapping. Precis. Agric. http://dx.doi.org/10.1007/s11119-016-9435-z.

Robinson, D.A., Lebron, I., Kocar, B., Phan, K., Sampson, M., Crook, N., Fendorf, S., 2010. Time-lapse geophysical imaging of soil moisture dynamics in tropical deltaic soils: an aid to interpreting hydrological and geochemical processes. Water Resour. Res. 46, 1–12. http://dx.doi.org/10.1029/2008WR006984.

Schneider, K., Huisman, J., Breuer, L., Zhao, Y., Frede, H., 2008. Temporal stability of soil moisture in various semi-arid steppe ecosystems and its application in remote sensing. J. Hydrol. 359, 16–29. http://dx.doi.org/10.1016/j.jhydrol.2008.06.016.

Soil Survey Staff, 1999, Soil Taxonomy: A Basic System of Soil Classification for Making and Interpreting Soil Surveys, second ed. NRCS USDA Agr. Hbk., 436. Washington, D.C.

Starks, P.J., Heathman, G.C., Jackson, T.J., Cosh, M.H., 2006. Temporal stability of soil moisture profile. J. Hydrol. 324, 400–411. http://dx.doi.org/10.1016/j.jhydrol.2005.09.024.

Taguas, E.V., Gómez, J.A., 2015. Vulnerability of olive orchards under the current CAP (Common Agricultural Policy) regulations on soil erosion: a study case in Southern Spain. Land Policy 42, 683–694. http://dx.doi.org/10.1016/j.landusepol.2014.09.001.

Vachaud, G., Passerat De Silans, A., Balabanis, P., Vauclin, M., 1985. Temporal stability of spatially measured soil water probability density function. Soil Sci. Soc. Am. J. 49, 822–828. http://dx.doi.org/10.2136/sssaj1985.03615995004900040006x.

Van Arkel, Z., Kaleita, A.L., 2014. Identifying sampling locations for field-scale soil moisture estimation using K-means clustering. Water Resour. Res. 50, 7050–7057.

Vanderlinden, K., Vereecken, H., Hardelauf, H., Herbst, M., Martínez, G., Cosh, M.H., Pachepsky, Y.A., 2012. Temporal stability of soil water contents: a review of data and analyses. Vadose Zone J. 11. http://dx.doi.org/10.2136/vzj2011.0178.

Vereecken, H., Huisman, J.A., Pachepsky, Y., Montzka, C., van der Kruk, J., Bogena, H., Weihermüller, L., Herbst, M., Martinez, G., Vanderborght, J., 2014. On the spatio-temporal dynamics of soil moisture at the field scale. J. Hydrol. 516, 76–96. http://dx.doi.org/10.1016/j.jhydrol.2013.11.061.

Whelan, B.M., McBratney, A.B., Minasny, B., 2002. Vesper 1.5 – spatial prediction software for precision agriculture. In: Robert PC, Rust RH, Larson WE. (Eds.) Precision Agriculture, Proceedings of the 6th International Conference on Precision Agriculture, ASA/CSSA/SSSA, Madison, Wisconsin.

Zhu, Q., Lin, H., Doolittle, J., 2010. Repeated electromagnetic induction surveys for determining subsurface hydrologic dynamics in an agricultural landscape. Soil Sci. Soc. Am. J. 74, 1750. http://dx.doi.org/10.2136/sssaj2010.0055.